US005414782A

United States Patent [19]

Carasso

[11] Patent Number: 5,414,782

[45] Date of Patent: May 9, 1995

[54] **PROCEDURE FOR DIGITAL IMAGE RESTORATION**

[75] Inventor: **Alfred S. Carasso**, North Potomac, Md.

[73] Assignee: **The United States of Amercia as represented by the Secretary of Commerce**, Washington, D.C.

[21] Appl. No.: **991,105**

[22] Filed: **Dec. 16, 1992**

[51] **Int. Cl.**[6] **G06K 9/40**

[52] **U.S. Cl.** **382/270**; 364/413.19; 382/128

[58] **Field of Search** 382/6, 54, 42; 364/413.13, 413.17, 413.19, 822

[56] **References Cited**

U.S. PATENT DOCUMENTS

4,315,318	2/1982	Kato et al.	382/6
4,329,588	5/1982	Barrett et al.	364/416
4,331,877	5/1982	Barrett et al.	364/414
4,633,504	12/1986	Wihl	382/54
4,758,304	7/1988	McNeil et al.	156/626
4,877,479	10/1989	McNeil et al.	156/626
4,903,205	2/1990	Hishinuma	382/6
4,907,156	3/1990	Doi et al.	382/6
4,947,323	8/1990	Smith	364/413.13
5,047,968	9/1991	Carrington et al.	382/54

OTHER PUBLICATIONS

N. S. Kopeika, "Spectral Characteristics of Image Quality for Imaging Horizontally Through the Atmosphere," Applied Optics, vol. 16 (1977), pp. 2422–2426.

R. Weber, "The Ground-Based Electro-Optical Detection of Deep-Space Satellites," Applications of Electronic Imaging Systems, SPIE, vol. 143 (1978), pp. 59–69.

N. S. Kopeika, "Imaging Through the Atmosphere for Airborne Reconnaissance," Optical Engineering, vol. 26 (1987), pp. 1146–1154.

J. D. Gonglewski et al., "Laboratory and Field Results in Low Light Postdetection Turbulence Compensation Using Self Referenced Speckle Holography," Digital Image Synthesis and Inverse Optics, SPIE, vol. 1351 (1990), pp. 798–806.

H. T. Yura, "Imaging in Clear Ocean Water," Applied Optics, vol. 12 (1973), pp. 1061–1066.

C. B. Johnson, "A Method for Characterizing Electro-Optical Device Modulation Transfer Functions," Photographic Science and Engineering, vol. 14 (1970), pp. 413–415.

C. B. Johnson, "Classification of Electron-Optical Device Modulation Transfer Functions," Advances in Electronics and Electron Physics, vol. 33B (1972), pp. 579–584.

C. B. Johnson et al., "High Resolution Microchannel Plate Image Tube Development," Electron Image Tubes and Image Intensifiers II, SPIE, vol. 1449 (1991), pp. 2–12.

F. C. Wagner et al., "A Characterization of the Scatter Point-Spread-Function in Terms of Air Gaps," IEEE Transactions on Medical Imaging, vol. 7 (1988), pp. 337–344.

(List continued on next page.)

Primary Examiner—Joseph Mancuso

Attorney, Agent, or Firm—Panitch Schwarze Jacobs & Nadel

[57] **ABSTRACT**

The image restoration system and method of the present invention is applied to point spread functions p(x,y) which may be described in the Fourier domain as

$$\hat{p}(\xi,\eta)=\exp\{-\Sigma_{i=1}^{J}\lambda_i(\xi^2+\eta^2)^{\beta_i}\},\quad \lambda_i\geqq 0,\quad 0<\beta_i\leqq 1,$$

to improve noise performance and permit identification of fine detail. The novel method formulates the image restoration problem as a problem in the partial differential equations describing diffusion phenomena using a new type of a priori constraint. The restored image is obtained by minimizing a quadratic functional incorporating this new constraint. The solution of the minimization problem may be obtained directly by means of fast Fourier transform algorithms. The restoration method may be performed as a sequence of partial restorations as $t\downarrow 0$ wherein the partial restorations become sharper and noisier as $t\downarrow 0$, or as a single full restoration. The sequence of partial restorations may reveal features of the image before such features become obscured by noise and may permit adjustment of the parameters characterizing the blurring functions and constraints.

12 Claims, 3 Drawing Sheets

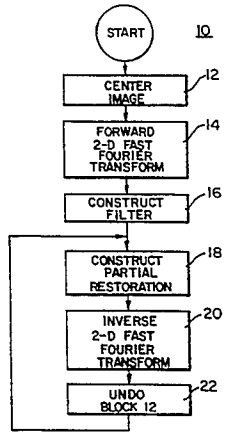

OTHER PUBLICATIONS

S. Webb et al., "Constrained Deconvolution of SPECT Liver Tomograms by Direct Digital Image Restoration," Medical Physics, vol. 12 (1985), pp. 53–58.

U. Raff et al., "Improvement of Lesion Detection in Scintigraphic Images by SVD Techniques for Resolution Recovery," IEEE Transactions on Medical Imaging, vol. MI-5 (1986), pp. 35–44.

B. C. Penney et al., "Constrained Least-Squares Restoration of Nuclear Medicine Images: Selecting the Coarseness Function," Medical Physics, vol. 14 (1987), pp. 849–858.

B. C. Penney et al., "Relative Importance of the Error Sources in Wiener Restoration of Scintigrams," IEEE Transactions on Medical Imaging, vol. 9 (1990), pp. 60–70.

K. S. Pentlow et al., "Quantitative Imaging of I-124 Using Positron Emission Tomography with Applications to Radioimmunodiagnosis and Radioimmunotherapy," Medical Physics, vol. 18 (1991), pp. 357–366.

S. M. Mohapatra et al., "Transfer Function Measurement and Analysis for a Magnetic Resonance Imager," Medical Physics, vol. 18 (1991), pp. 1141–1144.

S. Rudin et al., "Improving Fluoroscopic Image Quality with Continously Variable Zoom Magnification," Medical Physics, vol. 18 (1991), pp. 972–977.

E. L. Nickoloff et al., "A Simplified Approach for Modulation Transfer Function Determinations in Computed Tomography," Medical Physics, vol. 12 (1985), pp. 437–442.

F. F. Yin et al., "Measurement of the Presampling Modulation Transfer Function of Film Digitizers Using a Curve Fitting Technique," Medical Physics, vol. 17 (1990), pp. 962–966.

P. J. Papin et al., "A Prototype Amorphous Selenium Imaging Plate System for Digital Radiography," Medical Physics, vol. 14 (1987), pp. 322–329.

S. Sanada et al., "Comparison of Imaging Properties of a Computed Radiography System and Screen-Film Systems," Medical Physics, vol. 18 (1991), pp. 414–420.

H. Fujita et al., "A Simple Method for Determining the Modulation Transfer Function in Digital Radiography," IEEE Transactions on Medical Imaging, vol. 11 (1992), pp. 34–39.

M. Takahashi et al., "Digital TV Tomography: Description and Physical Assessment," Medical Physics, vol. 17 (1990), pp. 681–685.

Y. Higashida et al., "Dual-Film Cassette Technique for Studying the Effect of Radiographic Image Quality on Diagnostic Accuracy," Medical Physics, vol. 11 (1984), pp. 646–652.

H. Kuhn et al., "Imaging Characteristics of Different Mammographic Screens," Medical Physics, vol. 19 (1992), pp. 449–457.

N. V. Rao, "Development of High Resolution Camera Tube for 2000 Line TV System," Electron Image Tubes and Image Intensifiers, SPIE, vol. 1243 (1990), pp. 81–86.

R. Barden et al., "High Resolution MS-Type Saticon Pick-Up Tube with Optimized Electron Optical Properties," Electron Image Tubes and Image Intensifiers II, SPIE, vol. 1449 (1991), pp. 136–147.

K. A. Costello et al., "Imaging GaAs Vacuum Photodiode with 40% Quantum Efficiency at 530 nm," Electron Image Tubes and Image Intensifiers, SPIE, vol. 1243 (1990), pp. 99–106.

A. S. Carasso et al., "Digital Removal of Random Media Image Degradations By Solving the Diffusion Equation Backwards in Time," SIAM Journal on Numerical Analysis, vol. 15 (1978), pp. 344–367.

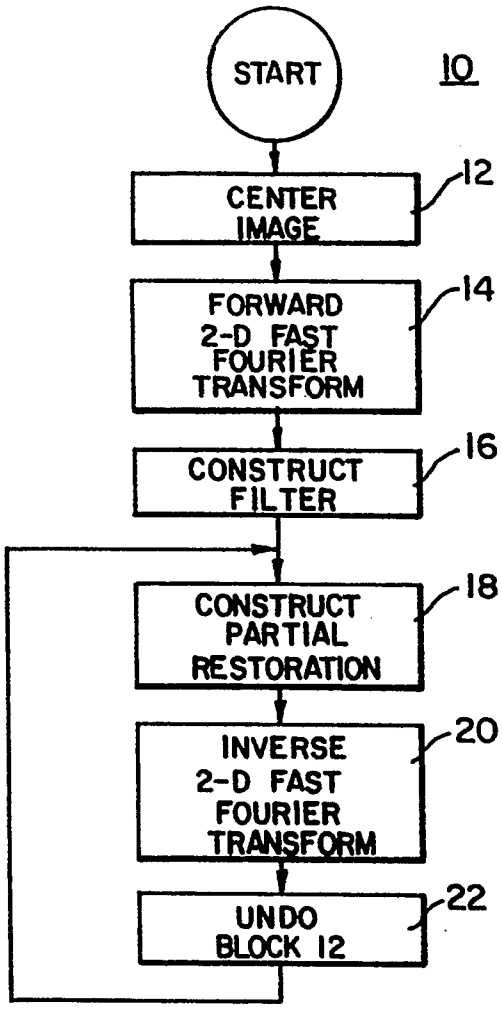
START
10
CENTER IMAGE
12
FORWARD 2-D FAST FOURIER TRANSFORM
14
CONSTRUCT FILTER
16
CONSTRUCT PARTIAL RESTORATION
18
INVERSE 2-D FAST FOURIER TRANSFORM
20
UNDO BLOCK 12
22

FIG. 1

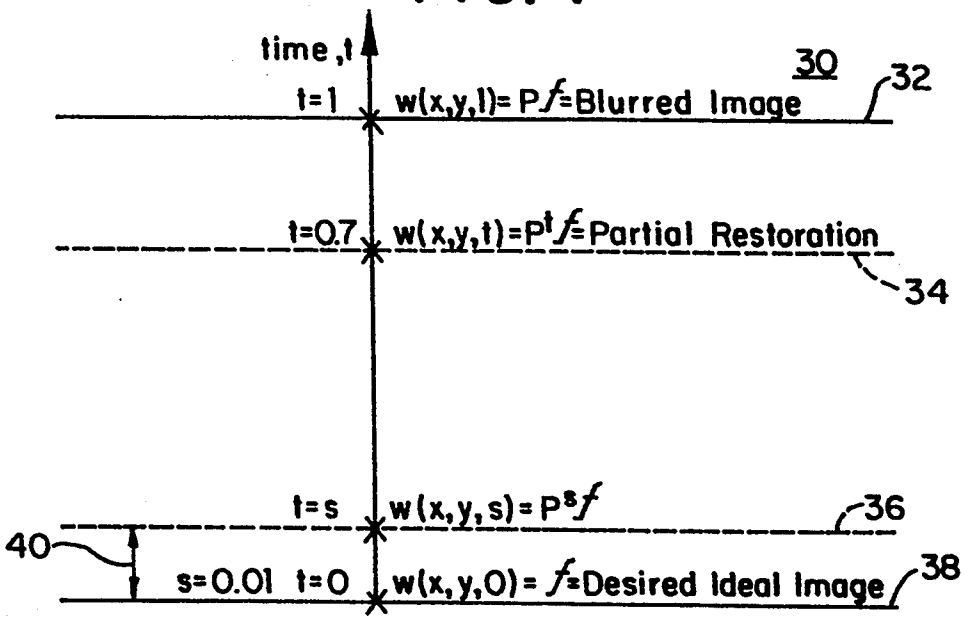
time, t
30
t=1
w(x,y,1)= Pf=Blurred Image
32
t=0.7
w(x,y,t)=P^t f=Partial Restoration
34
t=s
w(x,y,s)=P^s f
36
40
s=0.01
t=0
w(x,y,0)= f=Desired Ideal Image
38

FIG. 2

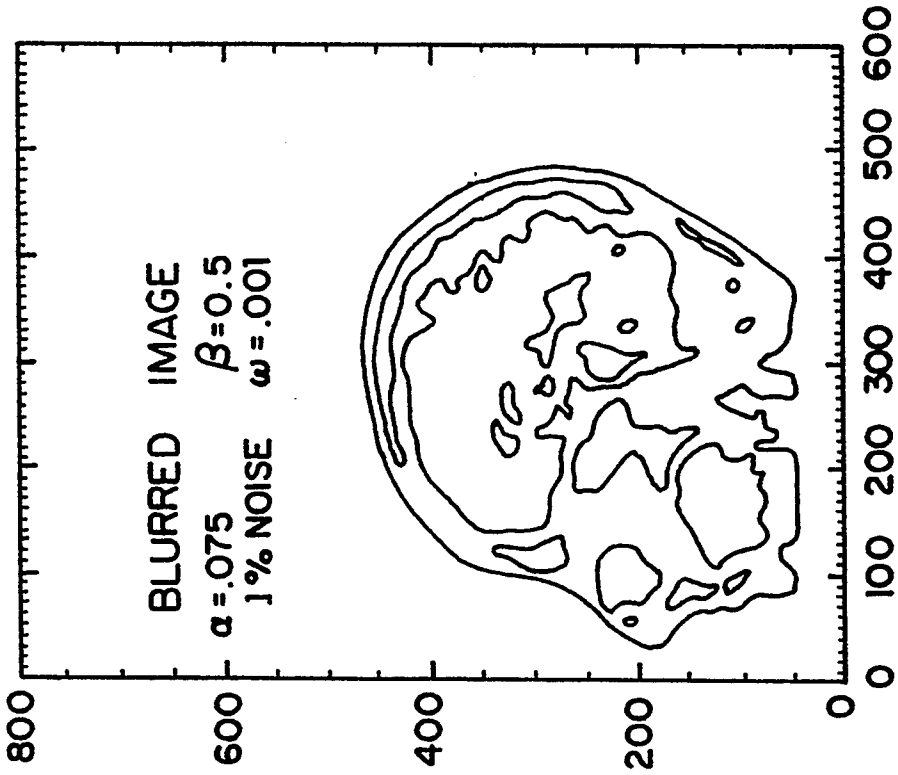
BLURRED IMAGE
α=.075
1% NOISE
β=0.5
ω=.001
800
600
400
200
0
0
100
200
300
400
500
600

FIG. 4

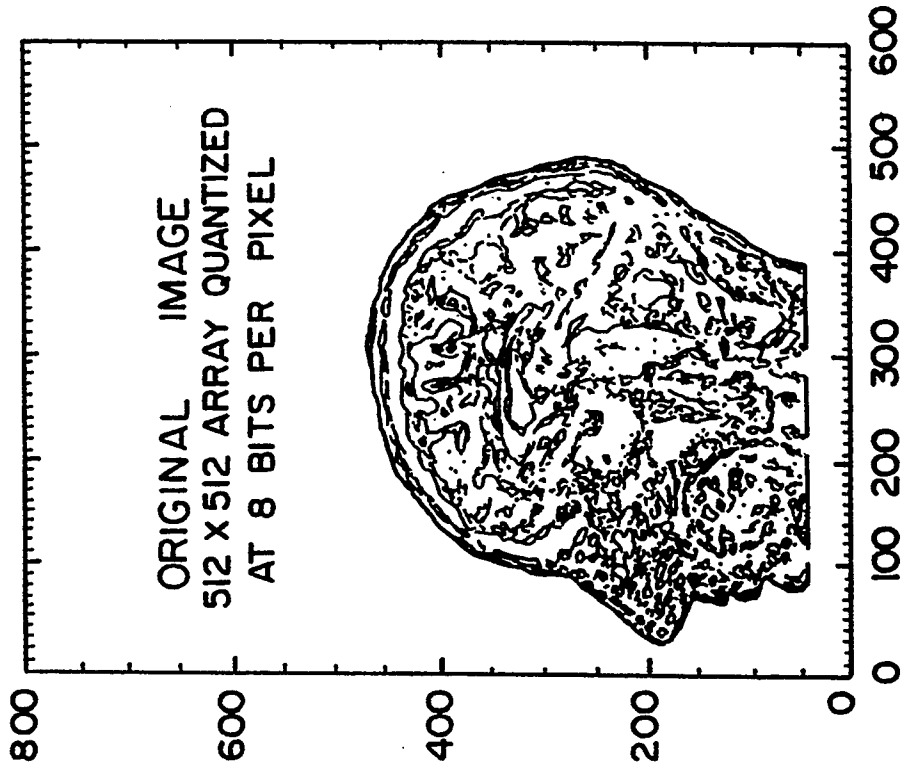
ORIGINAL IMAGE
512 X 512 ARRAY QUANTIZED
AT 8 BITS PER PIXEL
800
600
400
200
0
0
100
200
300
400
500
600

FIG. 3

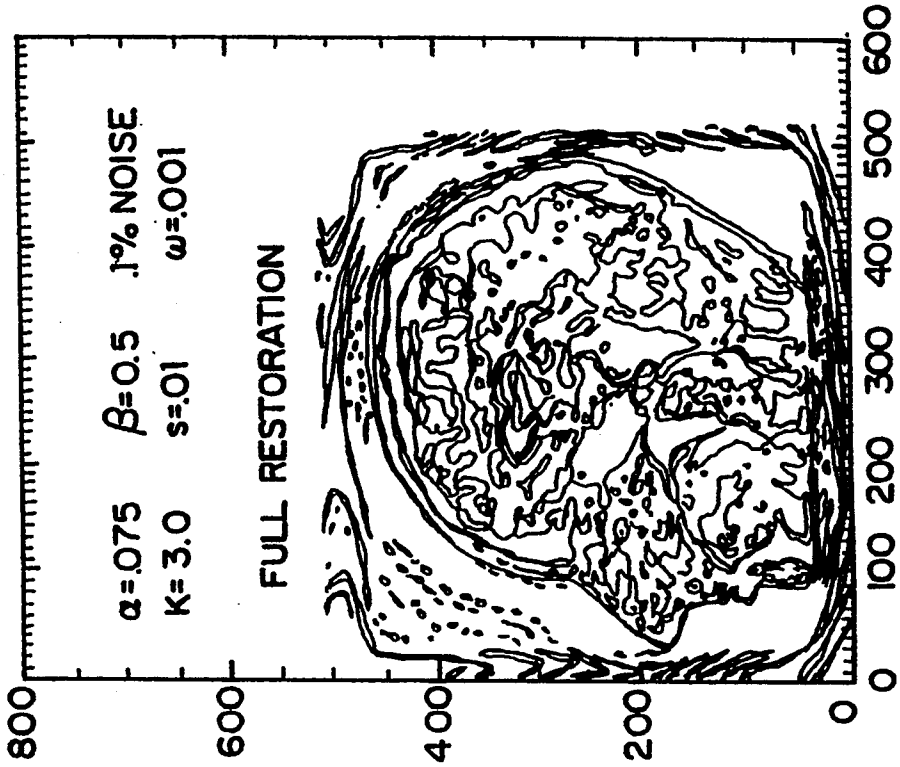
α=.075 β=0.5 .1% NOISE
K=3.0 s=.01 ω=.001
FULL RESTORATION
800
600
400
200
0
0 100 200 300 400 500 600

FIG. 6

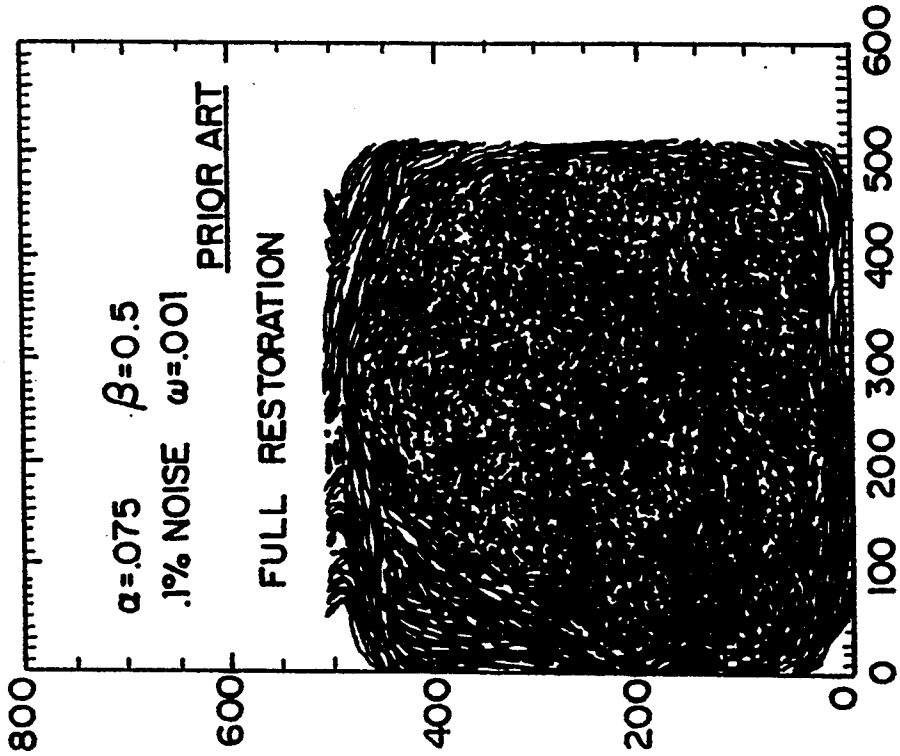
α=.075 β=0.5
.1% NOISE ω=.001
PRIOR ART
FULL RESTORATION
800
600
400
200
0
0 100 200 300 400 500 600

FIG. 5

PROCEDURE FOR DIGITAL IMAGE RESTORATION

BACKGROUND OF THE INVENTION

1. Field of the Invention

The present invention relates to image processing, and, in particular, to image restoration.

2. Statement of Related Art

Comprehensive coverage of prior art in the field of image restoration relevant to the system and method may be found in H. C. Andrews and B. R. Hunt, *Digital Image Restoration*, Prentice-Hall Signal Processing Series, Prentice-Hall, Inc., Englewood Cliffs, N.J. (1977); W. K. Pratt, *Digital Image Processing*, 2nd Edition, John Wiley and Sons, New York (1988); H. Stark, *Image Recovery, Theory and Application*, Academic Press, Inc., Harcourt Brace Jovanovich, Publishers, New York (1987); R. C. Gonzalez and P. Wintz, *Digital Image Processing*, 2nd Edition, Addison-Wesley Publishing Company, Inc., Advanced Book Program, Reading, Mass. (1987); and R. L. Lagendijk and J. Biemond, *Iterative Identification and Restoration of Images*, Kluwer International Series in Engineering and Computer Science, Kluwer Academic Publishers, Boston, Mass. (1991). For space-invariant blurs, digital image restoration is associated with the solution of two dimensional ill-posed convolution integral equations of the form

$$g(x,y) = \int_{-\infty}^{\infty}\int_{-\infty}^{\infty} p(x-u, y-v)f(u,v)dudv, \quad \text{Equation (1)}$$

where g(x,y) is the degraded image, f(x,y) is the desired ideal image, and p(x,y) is the known point spread function of the imaging system. The point spread function acts so as to blur or smooth out the ideal image, making it impossible to distinguish fine details in the recorded image g(x,y). Separately, g(x,y) is further contaminated by measurement noise. Thus:

$$g(x,y)=g_e(x,y)+n(x,y), \quad (2)$$

where $g_e(x,y)$ is the blurred image that would have been recorded in the absence of noise, and n(x,y) represents the cumulative effects of all noise processes affecting final acquisition of the digitized array g(x,y). This includes the case of multiplicative noise, where n(x,y) is a function of f(x,y). The noise component n(x,y) is unknown, but may be presumed small. Likewise, $g_e(x,y)$ is unknown. The type and intensity of the blurring caused by p, together with the magnitude of the noise in g, ultimately limit the quality of the restoration that can be achieved. It is convenient to write Equation (1) in operator notation as:

$$Pf=g, \quad (3)$$

where P is the integral operator in $L^2(R^2)$ with kernel p(x-u,y-v).

The two dimensional Fourier transform plays a major role in the subsequent analysis. For a function a(x,y) of the space variables x,y, the Fourier transform $\hat{a}(\xi,\eta)$ may be expressed as:

$$\hat{a}(\xi,\eta) = \int_{-\infty}^{\infty}\int_{-\infty}^{\infty} a(x,y)e^{-2\pi i(\xi x+\eta y)}dxdy. \quad \text{Equation (4)}$$

The Fourier transform of the point spread function is called the optical transfer function and is an important tool in image analysis. The convolution theorem states that the transform of a convolution is the product of the individual transforms. The Parseval theorem states that the L^2 scalar product of two functions in the space variables x,y is equal to their scalar product in the transform variables ξ,η. These and other results from Fourier analysis in L^2 are well known in the art. For convolution equations such as Equation (1), it is advantageous to perform the analysis and computations in the Fourier domain. After image processing, the inverse Fourier transform is used to return to the space variables x,y.

The class G of point spread functions, described by Equation (5A) below, plays a key role in several civilian and military applications, including biomedical imaging; night vision systems; undersea imaging; imaging through the atmosphere; remote sensing; high definition television; and industrial applications. Consider first the class of point spread functions p(x,y) described as follows in the Fourier transform domain:

$$\hat{p}(\xi,\eta)=e^{-\lambda(\xi^2+\eta^2)^{\beta}},\ \lambda>0,\ 0<\beta\leqq 1. \quad (5)$$

The case $\beta=1$ corresponds to a Gaussian point spread function. This case occurs in quite diverse applications, including undersea imaging (see H. T. Yura, 'Imaging in Clear Ocean Water,' *Applied Optics*, Vol. 12 (1973), pp. 1061–1066); low light-level electro-optical detection (see R. Weber, 'The Ground-Based Electro-Optical Detection of Deep-Space Satellites,' *Applications of Electronic Imaging Systems*, Proceedings of the Society of Photo-Optical Instrumentation Engineers, Vol. 143, R. E. Franseen and D. K. Schroder, Eds. (1978), pp. 59–69); nuclear medicine gamma camera scintigrams (see S. Webb et al., 'Constrained Deconvolution of SPECT Liver Tomograms by Direct Digital Image Restoration,' *Medical Physics*, Vol. 12 (1985), pp. 53–58; U. Raff et al., 'Improvement of Lesion Detection in Scintigraphic Images by SVD Techniques for Resolution Recovery,' *IEEE Transactions on Medical Imaging*, Vol. MI-5 (1986), pp. 35–44; B. C. Penney et al., 'Constrained Least Squares Restoration of Nuclear Medicine Images: Selecting the Coarseness Function,' *Medical Physics*, Vol. 14 (1987), pp. 849–859; B. C. Penney et al., 'Relative Importance of the Error Sources in Wiener Restoration of Scintigrams,' *IEEE Transactions on Medical Imaging*, Vol. 9 (1990), pp. 60–70; K. S. Pentlow et al., 'Quantitative Imaging of I-124 Using Positron Emission Tomography with Applications to Radioimmunodiagnosis and Radioimmunotherapy,' *Medical Physics*, Vol. 18 (1991), pp. 357–366); magnetic resonance imaging (see S. M. Mohapatra et al., 'Transfer Function Measurement and Analysis for a Magnetic Resonance Imager,' *Medical Physics*, Vol. 18 (1991), pp. 1141–1144); and computed tomography scanners (see E. L. Nickoloff and R. Riley, 'A Simplified Approach for Modulation Transfer Function Determinations in Computed Tomography,' *Medical Physics*, Vol. 12 (1985), pp. 437–442).

The case $\beta=5/6$ describes blurring caused by atmospheric turbulence under long time exposure. This optical transfer function is important in post processing of

degraded images obtained in airborne reconnaissance, in remote sensing from environmental or surveillance satellites, in the detection of deep-space satellites from ground-based telescopes, and in observational astronomy (see J. C. Wyant, Ed., *Imaging Through the Atmosphere*, Proceedings of the Society of Photo-Optical Instrumentation Engineers, Vol. 75 (1976); N. S. Kopeika, 'Spectral Characteristics of Image Quality for Imaging Horizontally Through the Atmosphere,' *Applied Optics*, Vol. 16 (1977), pp. 2422–2426; R. Weber, 'The Ground-Based Electro-Optical Detection of Deep-Space Satellites,' *Applications of Electronic Imagining Systems*, Proceedings of the Society of Photo-Optical Instrumentation Engineers, Vol, 143, R. E. Franseen and D. K. Schroder, Eds. (1978), pp. 59–69; N. S. Kopeika, 'Imaging Through the Atmosphere for Airborne Reconnaissance,' *Optical Engineering*, Vol. 26 (1987), pp. 1146–1154; J. D. Gonglewski and D. G. Voelz, 'Laboratory and Field Results in Low Light Post-detection Turbulence Compensation Using Self Referenced Speckle Holography,' *Digital Image Synthesis and Inverse Optics*, Proceedings of the Society of Photo-Optical Instrumentation Engineers, Vol. 1351, A. F. Gmitro, P. S. Idell, and I. J. LaHaie, Eds. (1990), pp. 798–806).

The case $\beta=\frac{1}{2}$ corresponds to the Cauchy or Lorentzian density, and may be used to describe X-ray scattering in radiology (see F. C. Wagner et al., 'A Characterization of the Scatter Point Spread Function in Terms of Air Gaps,' *IEEE Transactions on Medical Imaging*, Vol. 7 (1988), pp. 337–344).

A wide variety of electron-optical devices obey Equation (5) with a value of β satisfying $\frac{1}{2}\leqq\beta\leqq 1$ (see C. B. Johnson, 'A Method for Characterizing Electro-Optical Device Modulation Transfer Functions,' *Photographic Science and Engineering*, Vol. 14 (1970), pp. 413–415; C. B. Johnson, 'Classification of Electron-Optical Device Modulation Transfer Function,' *Advances in Electronics and Electron Physics*, Vol. 33B . (1972), pp. 579–584; C. B. Johnson et al., 'High-Resolution Microchannel Plate Image Tube Development,' *Electron Image Tubes and Image Intensifiers II*, Proceedings of the Society of Photo-Optical Instrumentation Engineers, Vol. 1449, I. P. Csorba, Ed. (1991), pp. 2–12).

Such devices constitute important elements of various biomedical imaging modalities, including image intensifier-video camera (II-TV) fluoroscopic systems (see S. Rudin et al., 'Improving Fluoroscopic Image Quality with Continuously Variable Zoom Magnification,' *Medical Physics*, Vol. 19 (1991), pp 972–977); radiographic film digitizers (see F. F. Yin et al., 'Measurement of the Presampling Transfer Function of Film Digitizers Using a Curve Fitting Technique,' *Medical Physics*, Vol. 17 (1990), pp. 962–966); radiographic selenium imaging plates (see P. J. Papin and H. K. Huang, 'A Prototype Amorphous Selenium Imaging Plate System for Digital Radiography,' *Medical Physics*, Vol. 14 (1987), pp. 322–329); computed radiography photostimulable phosphor systems (see S. Sanada et al., 'Comparison of Imaging Properties of a Computed Radiography System and Screen-Film Systems,' *Medical Physics*, Vol. 18 (1991), pp . 414–420; H. Fujita et al., 'A Simple Method for Determining the Modulation Transfer Function in Digital Radiography,' *IEEE Transactions on Medical Imaging*, Vol. 11 (1992), pp. 34–39); digital TV tomography systems (see M. Takahashi et al., 'Digital TV Tomography: Description and Physical Assessment,' *Medical Physics*, Vol. 17 (1990), pp. 681–685); and radiographic screen-film systems (see Y. Higashida et al., 'Dual-Film Cassette Technique for Studying the Effect of Radiographic Image Quality on Diagnostic Accuracy,' *Medical Physics*, Vol. 11 (1984), pp. 646–652; H. Kuhn and W. Knupfer, 'Imaging Characteristics of Different Mammographic Screens,' *Medical Physics*, Vol. 19 (1992), pp. 449–457).

Other important image tube/image intensifier applications include high definition television (HDTV) (see N. V. Rao, 'Development of a High-Resolution Camera Tube for 2000-Line TV System,' *Electron Tubes and Image Intensifiers*, Proceedings of the Society for Photo-Optical Instrumentation Engineers, Vol. 1243, I. P. Csorba, Ed. (1990), pp. 81–86; R. Barden et al., 'High Resolution MS-Type Saticon Pick-Up Tube with Optimized Electron-Optical Properties,' *Electron Tubes and Image Intensifiers II*, Proceedings of the Society for Photo-Optical Instrumentation Engineers, Vol. 1449, I. P. Csorba, Ed. (1991), pp. 136– 147), and night vision and undersea imaging systems (see K. A. Costello et al., 'Imagining GaAs Vacuum PhotoDiode with 40% Quantum Efficiency at 530 nm,' *Electron Tubes and Image Intensifiers*, Proceedings of the Society for Photo-Optical Instrumentation Engineers, Vol. 1243, I. P. Csorba, Ed. (1990), pp. 99–106.

In a typical imaging situation, several electron-optical devices may be cascaded together and used to image objects through a distorting medium such as the atmosphere or the ocean. The overall optical transfer function is then the product of finitely many functions of the type given by Equation (5), i.e.,

$$\hat{p}(\xi,\eta) = e^{-\sum_{i=1}^{J}\lambda^{i(\xi^2+\eta^2)\beta i}}, \quad \lambda_i \geqq 0, \quad 0 < \beta_i \leqq 1. \qquad \text{Equation (5A)}$$

Each factor in this product represents a component of the total blur, and is described by Equation (5) with a particular value for λ and β. A method for determining λ_i and β_i for each component is discussed in C. B. Johnson, 'Classification of Electron-Optical Device Modulation Transfer Function,' Advances in Electronics and Electron Physics, Vol 33B (1972), pp. 579–584. Equation (5A) also describes cascaded electron-optical devices forming the imaging chain in many digital radiography systems. Frequency domain characterization of such systems is an important and ongoing task, as is evident from the above-cited references. In several industrial applications, the general functional form defined by Equation (5A) may be found to best-fit an empirically determined optical transfer function, by suitable choices of the parameters λ_i, β_i and J.

It is emphasized that while many imaging phenomena do not have optical transfer functions that can be well-described by Equation (5A), the latter nevertheless encompasses a significant set of imaging problems. We denote by G the class of optical transfer functions defined by Equation (5A). Note that Equation (5) is a special case of Equation (5A). The functions in G are infinitely divisible probability density functions.

Most current approaches to image restoration are based on linear system inverse filter theory, where the input is the degraded image, and the single output is an approximation to the ideal image. Using a priori constraints on the unknown ideal image, various regularization methods are employed in these approaches, in order to stabilize the deconvolution procedure in the

presence of noise. Tikhonov regularization is one of the best-known examples of such procedures. This method is closely related to Wiener filtering. The Tikhonov regularization method is also known as constrained least squares. In its simplest form, Tikhonov restoration is based on the following a priori information concerning the unknown ideal image f(x,y) in Equation (1), and the noise n(x,y) in the degraded image g(x,y):

$$\|f\| \leqq M, \quad \|n\| \leqq \epsilon, \tag{6}$$

where $\| \ \|$ denotes the $L^2(R^2)$ norm. This leads to the following constrained restoration problem for Equation (3). Given ϵ, $M>0$, with $\epsilon/M<<1$, find all $f \in L^2(R^2)$ such that

$$\|Pf-g\| \leqq \epsilon, \ \|f\| \leqq M. \tag{7}$$

Let $\omega=\epsilon/M$. In this context, ω may be viewed as the L^2 noise-to-signal ratio. Tikhonov restoration provides a solution to Equation (7) by finding the function $f^T(x,y)$ which minimizes the Tikhonov functional:

$$\|Pf-g\|^2+\omega^2\|f\|^2, \tag{8}$$

over all f in L^2. Using the normal equations, $[P^*P+\omega^2I]f^T=P^*g$, where P^* is the Hilbert space adjoint of P, together with Fourier transforms, it is easily shown that $f^T(x,y)$ satisfies $pf^T=g^T$, where $g^T(x,y)$ is defined in the Fourier domain as follows:

$$\hat{g}^T(\xi,\eta)=\hat{g}(\xi,\eta)/[1+\omega^2|\hat{p}(\xi,\eta)|^{-2}]. \tag{9}$$

In particular, Tikhonov restoration may be understood to solve Equation (3) with a modified right hand side g^T, obtained by filtering g in the frequency domain with a specific low-pass filter. The filter is a function of ω and the known optical transfer function $\hat{p}(\xi,\eta)$. The Tikhonov solution may be obtained by inverse Fourier transforming $\hat{f}^T(\xi,\eta)=\hat{g}^T(\xi,\eta)/\hat{p}(\xi,\eta)$ The a priori bound constraint on $\|f\|$ in Equation (6) prevents explosive growth of noise in the restoration process. However, that constraint is not strong enough to prevent substantial noise contamination from obscuring fine detail in the restored image.

BRIEF DESCRIPTION OF THE DRAWINGS

FIG. **1** shows a flow chart representation of the image restoration method of the present invention;

FIG. **2** shows a graphical description of the constraint in Equation (13);

FIG. **3** shows a contour map representation of an original image;

FIG. **4** shows a contour map representation of a blurred image corresponding to the original image of FIG. **3**;

FIG. **5** shows a contour map representation of a restored image generated by applying the prior art Tikhonov restoration method to the blurred image of FIG. **4**; and

FIG. **6** shows a contour map representation of a restored image generated by applying the restoration method of the present invention to the blurred image of FIG. **4**.

DETAILED DESCRIPTION OF THE INVENTION

Referring now to FIG. **1**, a flow chart representation of image restoration method **10** of the present invention is shown. It will be understood that the particular form of the optical transfer function in Equation (5A) plays no role in Tikhonov restoration. Indeed, Tikhonov regularization may be applied to a much wider class of image restoration problems. However, the fact that point spread functions in class G are infinitely divisible probability density functions plays an essential role in image restoration method **10**. The blurred image g(x,y) is now viewed as the end result of a diffusion process applied to the desired ideal image f(x,y). This follows by recognizing Equation (5A) as the causal fundamental solution for the following parabolic initial value problem for the function w(x,y,t):

$$\frac{\partial w}{\partial t} = -\sum_{i=1}^{J} \gamma_i(-\Delta)^{\beta_i} w, \quad t>0, \quad x,y \in R^2 \qquad \text{Equation (10)}$$

$w(x,y,0)=f(x,y)$.

In Equation (10), $\gamma_i=\lambda_i(4\pi^2)^{-\beta_i}>0$, are the diffusion coefficients. If all $\beta_i=1$, Equation (10) is the classical heat equation. For $0<\beta_i<1$, Equation (10) represents a generalized diffusion process. Fourier analysis of Equation (10) shows that if Equation (3) holds with the kernel of P satisfying Equation (5A), then the blurred noiseless image $g_e(x,y)$ is the solution of Equation (10) at $t=1$,

$$g_e(x,y)=w(x,y,1) \tag{11}$$

For any t with $0 \leqq t \leqq 1$, Fourier analysis may be used to define the fractional powers p^t of the integral operator P when its kernel satisfies Equation (5A). The kernel of p^t is the optical transfer function given by Equation (5A) with λ_i replaced by $t\lambda_i$. Moreover, $p^tp^r=p^{t+r}$ for any $t,r \geqq 0$ and $p^0=I$, where I is the identity operator on $L^2(R^2)$. The forward solution of Equation (10) is given by $w(x,y,t)=p^tf$. Consequently, for point spread functions in class G, image restoration is exactly equivalent to solving the partial differential equation problem in Equation (10) backwards in time, using the given degraded image g(x,y), rather than $g_e(x,y)$, as data at $t=1$. The desired ideal image is the corresponding solution at $t=0$,

$$f(x,y)=w(x,y,0) \tag{12}$$

For any t with $0<t<1$, w(x,y,t) constitutes a partial restoration, while w(x,y,0) is the full restoration. In the absence of noise, with data $g_e(x,y)$ in place of g(x,y), w(x,y,t) closely approximates f(x,y), provided t is sufficiently small, the λ_i are small, and f(x,y) is sufficiently well-behaved, i.e., high frequency components do not dominate the power spectrum of f(x,y). This is likely to be the case in the vast majority of images f(x,y) encountered in practical applications.

Thus, if $n(x,y)=0$ in Equation (2), then for some fixed small $s>0$, and a small constant δ, the inequality $\|w(.,s)-f\| \leqq \delta$, holds. When $n(x,y) \neq 0$, such an inequality is not true because spurious high frequency noise artifacts can seriously contaminate the restoration process as $t \downarrow 0$. However, in the presence of noise, such an inequality may be imposed as an additional constraint. In this case, noise artifacts in the restored image may be expected to be substantially reduced.

Since $\|n\| \leqq \epsilon$, it is convenient to put $\delta=K\epsilon$ for some small constant $K>0$. With $w(x,y,s)=P^sf$, this new constraint may then be expressed as follows: For fixed

small $s>0$ and small constant $K>0$, where both s and K are determined on the basis of a priori information,

$$\|(I-P^s)f\| \leqq K\epsilon. \tag{13}$$

Referring now to FIG. 2, there is shown graphical representation **30** of the constraint in Equation (13). The desired ideal image f(x,y) corresponds to w(x,y,0), the data at time $t=0$ in the partial differential equation problem, Equation (10). This corresponds to line **38** of representation **30**. It will be understood that line **38** corresponds to If of Equation (13). The blurred noiseless image, $g_e(x,y)=Pf=w(x,y,1)$, is the corresponding solution at time $t=1$ as shown at line **32**. At any intermediate time t with $0<t<1$, $w(x,y,t)=p^t f$ is a partial restoration, becoming the full restoration f, as $t \downarrow 0$. An example is shown at line **34** wherein $t=0.7$.

If $g_e(x,y)$ could be used as data at $t=1$ in the time-reversed problem, then for small $s>0$, $w(x,y,s)=P^s f$ would be a good approximation to f, i.e., $\|f-P^s f\|$ would be a small quantity. An example $t=s$ for a small value of s is shown at line **36**. In reality, one must use the noisy image g(x,y) as data at $t=1$. In that case, high frequency noise amplification in the Tikhonov restoration process causes $w(x,y,s)=P^s f$ to differ appreciably from f. In the present invention, the requirement that $\|f-P^s f\|$ be small is enforced as an explicit additional constraint, in Equation (13). An example with the explicit choice $s=0.01$ is indicated as reference numeral **40** in FIG. 2. This explicit requirement results in greatly reduced noise amplification.

Returning to the original problem, Equation (3), with the optical transfer function given by Equation (5A), a new constrained problem may be formulated. Given ϵ, M, K, $s>0$, with $s<1$ and $(\epsilon/M)<1$, find all $f \in L^2(R^2)$ such that

$$\|Pf-g\| \leqq \epsilon, \quad \|f\| \leqq M, \quad \|(I-P^s)f\| \leqq K\epsilon. \tag{14}$$

In an analogy with Tikhonov restoration, a solution to the new constrained problem may be determined by finding that function $f^c(x,y)$ which minimizes the functional of the present invention:

$$\|Pf-g\|^2+\|(\epsilon/M)f+(1/K)(I-P^s)f\|^2, \tag{15}$$

over all f in L^2. With $\omega=\epsilon/M$, $\mu=1/(1+K\omega)$ and $B=I-\mu P^s$, the functional of the present invention may be written more compactly as

$$\|Pf-g\|^2+(1/\mu K)^2\|Bf\|^2. \tag{16}$$

As before, the normal equations $[P^*P+(1/\mu K)^2 B^*B]f^c=P^*g$, combined with Fourier analysis, show that $Pf^c=g^c$, with $g^c(x,y)$ defined as follows in the Fourier domain:

$$\hat{g}^c(\xi,\eta)=\hat{g}(\xi,\eta)/[1+(1/\mu K)^2|\hat{p}(\xi,\eta)|^{-2}(1-\mu\hat{p}(\xi,\eta)^{s})^2]. \tag{17}$$

Image restoration method **10** of the present invention is performed by inverse Fourier transforming $\hat{f}^c(\xi,\eta)=\hat{g}^c(\xi,\eta)/\hat{p}(\xi,\eta)$. Note that with $s=0$, the new constraint set forth in Equation (13) is automatically satisfied. In that case, the inventive functional in Equation (15) reduces to the Tikhonov functional in Equation (8). At the same time, since $\omega=(1-\mu)/\mu K$, the inventive filter in Equation (17) reduces to the Tikhonov filter in Equation (9). Thus, $f^c(x,y)=f^T(x,y)$ if $s=0$. However, $f^c(x,y)\neq f^T(x,y)$ when $s>0$, as the two filters are then markedly different in their behavior at intermediate and high frequencies.

It will be understood that restoration procedures for point spread functions in class G may be mathematically compared. Furthermore, for point spread functions in class G, the fact that the new constraint in Equation (13) leads to a better restoration than does the constraint in Equation (6), can be proved mathematically. The improvement may be shown on the basis of error bounds for the restoration, as a function of the L^2 noise level ϵ in the degraded image g(x,y). It is useful in this proof to estimate the error in the partial restorations, $p^t f$ at any value of t with $0 \leqq t \leqq 1$. Consider first the Tikhonov restoration of the prior art. Let f(x,y) be any solution of the constrained restoration problem, Equation (7), with optical transfer function given by Equation (5A), and let $f^T(x,y)$ be the Tikhonov restoration. Then,

$$\|P^t(f-f^T)\| \leqq (1+\sqrt{2})M^{1-t}\epsilon^t, \quad 0 \leqq t \leqq 1. \tag{Equation (18)}$$

The inequality in Equation (18) is obtained using logarithmic convexity theorems for the related diffusion equation, Equation (10), and is understood by those skilled in the art to be best-possible. See Theorem 2 in Alfred S. Carasso et al., 'Digital Removal of Random Media Image Degradations by Solving the Diffusion Equation Backwards in Time,' *SIAM Journal on Numerical Analysis*, Vol. 15, (1978), pp. 344–367. Thus, a stronger error bound in the L^2 norm cannot be obtained for the constrained restoration problem in Equation (7). The behavior of the Tikhonov error as $t \downarrow 0$ is of major concern. If $\epsilon=10^{-4}$ in Equation (6), then $\epsilon^t=10^{-0.04}\approx 0.912$ at $t=0.01$. The inequality in Equation (18) implies a systematic loss of significant information as $t \downarrow 0$. In particular, at $t=0$, we have $\|f-f^T\| \leqq (1+\sqrt{2})M$. Thus, although the difference between f and f^T is bounded, there is no guarantee that noise artifacts in the Tikhonov restoration are necessarily small.

However, in image restoration process **10** of the present invention, the following result may be proven. Let f(x,y) be any solution of the new constrained restoration problem, Equation (14), with an optical transfer function given by Equation (5A) and let $f^c(x,y)$ be the restoration of an image according to image restoration method **10**. Then,

$$\|P^t(f-f^C)\| \leqq 2\sqrt{5}\,\Gamma^{1-t}\epsilon, \quad 0 \leqq t \leqq 1, \tag{Equation (19)}$$

where F is the unique solution of the transcendental equation $z=K+z^{1-s}$, and $1<\Gamma<<M/\epsilon$, provided $s>>s^*=K\epsilon/(M\,\mathrm{Log}(M/\epsilon))$.

The significant difference between the results of Equation (18) and the results of Equation (19) is that ϵ rather than ϵ^t appears on the right hand side of the inequality in Equation (19). This is the result of the additional constraint, Equation (13), which greatly reduces the possibility that spurious high frequency noise components in the data g(x,y) will contaminate the restoration near $t=0$. Thus, with $M=10$, $\epsilon=10^{-4}$, $s=0.01$, and $K=3$, it will be understood that $\Gamma\approx 72$ and that $\|f-f^c\| \leqq 0.0322$. However, it will also be understood that $\|f-f^T\| \leqq 24.2$. In this example, the error bound in the restoration according to image restoration method **10** is approximately seven hundred fifty times

smaller than that for the Tikhonov restoration of the prior art, provided the desired image satisfies Equation (13).

Computational implementation of image restoration method **10** will be understood by those skilled as follows. The essential idea in the implementation of image restoration method **10** is the use of the discrete Fourier transform to mimic the operations described above in the continuous Fourier transform domain. These computations are fast because of the use of the fast fourier transform to implement discrete Fourier transform operations. The close connection between the continuous and discrete Fourier transforms, under appropriate conditions, is taught in detail in E. O. Brigham, The Fast Fourier Transform, Prentice-Hall, Inc., Englewood Cliffs, N.J., (1974).

Method **10** of the present invention may be performed upon the degraded image $g(x_j,y_k)$ expressed as a digitized $N\times N$ array, where N is a power of 2, and where j,k are integers with $0\leqq j, k\leqq N-1$. With l the width of the image, let $\Delta x=\Delta y=1/N$ be the sampling interval, so that $x_j=j\Delta x$, $y_k=k\Delta y$. The actual image transformed by image restoration method **10** is assumed to be surrounded by a border of zeroes of sufficient width to eliminate wrap-around errors in discrete convolutions. The $N\times N$ array includes the actual image and its border. The optical transfer function for the imaging process is assumed given by Equation (5A) with known λ_i and β_i. Likewise, the positive constants ϵ, M, K, and s in Equation (14) are assumed to be known on the basis of a priori information.

Referring again to FIG. **1**, reference is made to the identifying numerals of the representation of image restoration method **10** of the present invention. As shown in centering block **12** of image restoration method **10**, the first step is to center the origin in the frequency array. This may be done by forming:

$$g(x_j,y_k)=(-1)^{j+k}g(x_j,y_k),\ 0\leqq j,k\leqq N-1$$

In forward transform block **14** a forward two-dimensional fast Fourier transform is performed upon $g(x_j,y_k)$ as determined in centering block **12**. The fast fourier transform of block **14** may be performed by forming:

$$G(\xi_m,\eta_n)=\Delta x\Delta y\Sigma_{j=0}^{N-1}\Sigma_{k=0}^{N-1}g(x_j,y_k)\exp\{-2\pi i(mj+nk)/N\},$$

where $0\geqq m,n\geqq N-1$ and $\xi_m=(m-N/2)/l, \eta_n=(n-N/2)/l$, $l=N\Delta x$.

The inventive filter of image restoration method **10** is then constructed in Fourier space as represented by filter construction block **16**. This filter is constructed with known λ_i, β_i, ϵ, M, K, $s>0$. In order to construct the novel filter of image restoration method **10** let $\omega=\epsilon/M$, $\mu=1/(1+K\omega)$, and let

$$p_{mn}=\exp\{-\Sigma_{i=1}^{J}\lambda_i(\xi_m^2+\eta_n^2)^{\beta i}\},\ \text{for } 0\leqq m, n\leqq N-1.$$

Then form:

$$G(\xi_m,\eta_n)=p_{mn}^2G(\xi_m,\eta_n)/\{p_{mn}^2+(1/\mu K)^2(1-\mu p_{mn}^s)^2\},$$

where $0\leqq m, n\leqq N-1$.

In partial restoration block **18** of image restoration method **10**, a partial restoration at t, $0\leqq t\leqq 1$, is constructed by forming:

$$G(\xi_m,\eta_n)=p_{mn}^{t-1}G(\xi_m,\eta_n),$$

where $0\leqq m, n\leqq N-1$.

In inverse transform block **20** an inverse two-dimensional fast Fourier transform is performed upon $G(\xi_m,\eta_n)$ which was constructed in restoration block **18**. The inverse transform shown in inverse transform block **20** may be obtained by forming

$$f(x_j,y_k,t)-l^{-2}\Sigma_{m=0}^{N-1}\Sigma_{n=0}^{N-1}G(\xi_m,\eta_n)\exp\{2\pi i(mj+nk)/N\},$$

where $0\leqq j, k\leqq N-1$. The centering of centering block **12** is then undone in block **22** of image restoration method **10** by forming

$$f(x_j,y_k,t)=(-1)^{j+k}f(x_j,y_k,t),$$

where $0\leqq j,k\leqq N-1$. Execution of image restoration method **10** may then return to partial restoration block **18** for any other desired value of t.

The result of performing the operations of block **22** is a partial restoration of an image according to image restoration method **10** at the preselected value of t. The user of image restoration method **10** may dispense with partial restoration and proceed directly to full restoration by setting $t=0$ when restoration block **18** is executed.

The scaling of the fast Fourier transforms in blocks **14**, **20** was chosen so as to correspond to continuous Fourier transform operations in a manner well known to those skilled in the art. However, the factor $\Delta x\Delta y$ may be omitted from the forward transform block **14** provided l^{-2} is replaced with N^{-2} in reverse transform block **20**. It is straightforward to modify the procedure so as to handle rectangular $N_1\times N_2$ images; see e.g., R. C. Gonzalez and P. Wintz, Digital Signal Processing, Second Edition, Addison-Wesley, Reading, Mass. (1987).

The system of method **10** may be implemented with tentative values of some of the parameters λ_i, β_i, ϵ, M, K, s. Image restoration method **10** may be repeated with adjusted values. A sequence of partial restorations as $t\downarrow 0$ is a useful option in that context because noise and ringing usually increase as $t\downarrow 0$. Thus, by performing the restoration in 'slow-motion,' an experienced user may more easily determine the influence of various parameter values and more quickly arrive at corrected values. Tikhonov restoration is obtained by setting $s=0$ in filter construction block **16**.

Image restoration method **10** may be experimentally verified in the following manner. In a simulation of blurring caused by X-ray scattering, an undegraded phantom image $f(x_j,y_k)$ was artificially blurred by convolution with an optical transfer function given by Equation (5). The image, shown in FIG. **3**, consisted of a five hundred twelve by five hundred twelve array, quantized at eight bits per pixel. Blurring was accomplished in the Fourier domain, by multiplying $F(\xi_m,\eta_n)$, obtained as in forward transform block **14** above by $q_{mn}=\exp\{-\alpha([l\xi_m]^2+[l\eta_n]^2)^\beta\}$, where $\alpha=0.075$ and $\beta=0.5$. An inverse Fast Fourier Transform, followed by the operations of block **22**, produces the blurred substantially noiseless image $g_e(x_j,y_k)$ in Equation (2).

Multiplicative noise was simulated by adding 0.1% uniformly distributed random noise to g_e. Thus, $n(x_j,y_k)=0.001v_{jk}g_e(x_j,y_k)$, where v_{jk} is a random num-

ber drawn from a uniform distribution in the range [−1,1]. This yields $\|n\| \leqq \epsilon \leqq 0.001 \|g_e\|$. Further, since $\|g_e\| \leqq \|f\|$, we find $\omega = \epsilon \|f\|^{-1} \leqq 0.001$. The value $g(x_j,y_k) = g_e(x_j,y_k) + n(x_j,y_k)$ is referred to as the blurred image. The blurred image is shown in FIG. 4.

Tikhonov restoration was applied to the blurred image using $\omega = 0.001$. The full restoration was contaminated by noise artifacts that made it impossible to visualize the image. See FIG. 5. A sequence of partial Tikhonov restorations was obtained at t=0.35, t=0.25, t=0.15, t=0.005, in addition to the full restoration at t=0. It will be understood that the partial restorations became sharper and noisier as $t \downarrow 0$. One may use the evolution as $t \downarrow 0$ to identify features that become obscured by noise at t=0. The growing influence of noise as $t \downarrow 0$ is a reflection of the $O(\epsilon^t)$ error bound characteristic of Tikhonov regularization as shown in Equation (18).

Image restoration method **10** was applied to the same blurred image, using $\omega = 0.001$, K=3, and s=0.01. In view of the conservatively small value for s, the assumption that f satisfies Equation (13) is sound. Indeed, the full restoration is now found to be relatively free from noise, and to provide substantial improvement over the full prior art Tikhonov restoration. See FIG. 6. This is in accordance with Equation (19) in Theorem 2. The sequence of partial restorations at t=0.35, t=0.25, t=0.15, and t=0.05 in image restoration method **10** is likewise found to be better behaved than the corresponding prior art Tikhonov sequence.

The above experiment illustrates the preceding theoretical developments set forth with respect to image restoration method **10**. At the same time, the experiment demonstrates the soundness of the computational implementation. Thus, image restoration method **10** may be reduced to practice as shown, for point spread functions in class G.

It is believed that image restoration method **10** may be advantageously applied in biomedical imaging, night vision systems, undersea imaging, imaging through the atmosphere, remote sensing, high definition television, as well as several other scientific and industrial applications where electron optics and class G point spread functions play a major role. Two key ideas make image restoration method **10** useful as a diagnostic tool in these and other fields. First, the substantial qualitative improvement in the full restoration that results from the additional constraint in Equation (13). Second, the display of the evolution of the restoration as t approaches 0. Together, these factors offer the possibility of greatly improved diagnostic capabilities, and provide a useful addition to current image restoration technology.

It is believed that method **10** is useful in this manner because it is based on mathematical tools which are different from prior art restoration algorithms. In contrast to the input-output linear system theory familiar to researchers with backgrounds in electrical engineering or computer science, and exemplified by Tikhonov restoration or Wiener filtering, method **10** is based upon partial differential equations, semi-group theory, and the mathematics of diffusion phenomena. The two key ideas mentioned in the preceding paragraph stem from this particular mathematical basis.

It will be understood that method **10** may be implemented on a general purpose computer programmed to perform the operations of blocks **12–22**. Alternately method **10** may be performed using dedicated conventional hardware to perform such conventional operations as the transforms of blocks **14**, **20**. Additionally it will be understood by those skilled in the art that dedicated hardware may be provided, using conventional synthesis and fabrication techniques, for performing other operations within method **10**.

I claim:

1. An image restoration method in a system having an image sensor and a digitizer, comprising the steps of:

(a) providing an imaging system described by an integral operator P;

(b) transmitting an ideal image f(x,y) through an image blurring and degrading transmission medium to provide a degraded image g(x,y) wherein the degraded image g(x,y) may be represented as Pf=g;

(c) receiving said degraded image g(x,y) from said transmission medium by said image sensor;

(d) digitizing said degraded image g(x,y) by said digitizer;

(e) transforming said degraded image g(x,y) to provide a time modified representation $w(x,y,t) = P^t f$ wherein $w(x,y,0) = P^0 f$ represents the ideal image f(x,y) at time t=0 prior to the operation of the integral operator P upon f and w(x,y,1)=Pf=g represents the degraded image g(x,y) when the image is received by said image sensor;

(f) requiring the magnitude of the difference between the ideal image f and a blurred version of f to be less than a preassigned tolerance value by minimizing $\|f - P^s f\|$ wherein $P^s f$ represents an image at time t=s as s approaches 0;

(g) determining a plurality of values of w(x,y,t) in accordance with said minimizing;

(h) adjusting said image in accordance with said determined plurality of values to provide a plurality of adjusted images;

(i) selecting an adjusted image of said plurality of adjusted images; and

(j) displaying said selected image.

2. The image restoration method of claim **1**, comprising the further steps of:

displaying a sequence of partially restored images represented as w(x,y,t) for a plurality of values of t as t approaches 0; and

determining an optimum image of said plurality of partially restored images in accordance with said displayed sequence.

3. The image restoration method of claim **1**, wherein said constraining comprises the step of imposing the constraint $\|f - P^s f\| \leqq K\epsilon$, where K is a constant and ϵ is representative of at least one image restoration parameter.

4. The image restoration method of claim **3**, comprising the further step of imposing the constraint $\|Pf - g\| \leqq \epsilon$, wherein ϵ is representative of at least one image restoration parameter.

5. The image restoration method of claim **4**, comprising the further step of imposing the constraint $\|f\| \leqq M$, wherein $M >> \epsilon$.

6. The image restoration method of claim **5**, comprising the further step of determining a restored image f(x,y) which minimizes the quantity

$$\{\|Pf - g\|^2 + \|(\epsilon/M)f + (1/K)(f - P^s f)\|^2\}.$$

7. The image restoration method of claim **6**, wherein a plurality of images $w(x,y,t) = P^t f$ are determined for a corresponding plurality of values of the time t.

8. The image restoration method of claim 7, wherein said plurality of values of time comprises a sequence of progressively smaller values.

9. The image restoration method of claim 8, wherein the values of said restoration parameters are adjusted in accordance with said plurality of images for successively smaller values of time.

10. The image restoration method of claim 7, wherein each image $w(x,y,t)=P^t f$ is determined in the Fourier Transform domain by $\hat{w}(\xi,\eta,t)=\hat{p}(\xi,\eta)^t\hat{f}(\xi,\eta)$, wherein $\hat{w}(\xi,\eta,t)$ is the Fourier transform of w (x,y,t , $\hat{p}(\xi,\eta)$ is an optical transfer function of said system, and $\hat{f}(\xi,\eta)$ is the Fourier transform of f(x,y).

11. The image restoration method of claim 6, wherein said restored image f(x,y) is determined through algebraic operations performed in the Fourier Transform domain.

12. The image restoration method of claim 1, wherein $\hat{f}(\xi,\eta)$, the Fourier Transform of f(x,y), is determined by $\hat{f}(\xi,\eta)=\hat{g}(\xi,\eta)/\{\hat{p}(\xi,\eta)[1+(\mu K|\hat{p}(\xi,\eta)|)^{-2}(1-\mu\hat{p}(\xi,\eta)^{s})^2]\}$, wherein $\hat{g}(\xi,\eta)$ is the Fourier Transform of the degraded image g(x,y), $\hat{p}(\xi,\eta)$ is an optical transfer function of said system, ϵ is representative of at least one constant, K is a constant, $\mu=(1+K\epsilon/M)^{-1}$, $M>>\epsilon$ and s is a substantially small value of time.

* * * * *